ELSEVIER

Combustion and Flame 132 (2003) 352–363

Combustion and Flame

Effects of dimethyl methylphosphonate on premixed methane flames

M.F.M. Nogueira[1], E.M. Fisher*

Sibley School of Mechanical and Aerospace Engineering, Cornell University, Ithaca, NY, USA

Received 3 July 2001; received in revised form 27 June 2002; accepted 9 August 2002

Abstract

The impact of dimethyl methylphosphonate (DMMP) was studied in a premixed methane/oxygen/N_2-Ar flame in a flat flame burner slightly under atmospheric pressure at two different equivalence ratios: rich and slightly lean. CH_4, CO, CO_2, CH_2O, CH_3OH, C_2H_6, C_2H_4, and C_2H_2 profiles were obtained with a Fourier Transform Infrared (FTIR) spectrometer. Gas samples, analyzed in the FTIR, were extracted from the reaction zone using a quartz microprobe with choked flow at its orifice. Temperature profiles were obtained by measuring the probe flow rate through the choked orifice. Flame calculations were performed with two existing detailed chemical kinetic mechanisms for organophosphorus combustion. DMMP addition caused all profiles except that of CH_3OH to move further away from the burner surface, which can be interpreted as a consequence of a reduction in the adiabatic flame speed. Experimentally, the magnitude of the shift was 50% greater for the near-stoichiometric flame than for the rich flame. Experimental CH_3OH profiles were four to seven times higher in the doped flames than in the undoped ones. The magnitude of this effect is not predicted in the calculations, suggesting a need for further mechanism development. Otherwise, the two mechanisms are reasonably successful in predicting the effects of DMMP on the flame.

Keywords: Flame inhibition, Organophosphorus, Microprobe, FTIR, Flat-flame burner, Premixed flame, Detailed chemical kinetic modelling

1. Introduction

Interest in combustion chemistry of organophosphorus compounds has been motivated by two applications: incineration of chemical warfare agents and fire suppression. The US and Russia have agreed to destroy all obsolete chemical warfare agents including organophosphorus nerve agents, and the National Research Council has endorsed incineration as a means of destroying the stockpiles [1]. Research has been performed both in the US and in Russia to investigate flame [2–9] and pyrolysis [10–12] chemistry of simulants of nerve agents that are not highly toxic, including dimethyl methylphosphonate (DMMP). Phosphorus-containing compounds have recently attracted interest as potential replacements for ozone-depleting halon fire suppressants, the production of which has been banned under the Montreal Protocol and its amendments [13,14].

Both fire suppression and chemical weapon incineration applications would benefit from a reliable detailed chemical kinetic mechanism for combustion of organophosphorus compounds. Two mechanisms have recently been proposed for organophosphorus combustion [15,16], but they have been validated

* Corresponding author: Tel.: +1-607-255-8309; fax: +1-607-255-9410.

E-mail address: emf4@cornell.edu (E.M. Fisher).

[1] Permanent address: Campus Universitário do Guamá, Dept. of Mechanical Engineering, Universidade Federal do Pará, Belém-PA Brazil.

0010-2180/03/$ – see front matter
doi:10.1016/0010-2180(02)00464-9

against only limited experimental data. In the present work these mechanisms are tested against experimental data under flame conditions that are realistic for flame suppression and incineration: combustion with methane in a nitrogen/oxygen environment at near-ambient pressure.

Most previous DMMP combustion experiments yielding species data have involved low-pressure hydrogen/oxygen/argon flames. Korobeinichev et al. [3,5] and Werner and Cool [2] both used molecular-beam mass spectrometry to study the structure of premixed stoichiometric H_2/O_2/Ar flat flames doped with DMMP, between 40 and 80 torr. They were able to measure DMMP and various stable and unstable products and intermediates. Temperature was measured by thermocouple. DMMP loading was between 1000 and 11,000 ppm. Both sets of investigators observed substantial increases in post-flame temperature (approximately 300°K) with the addition of DMMP. Species measurements differed in some respects: certain intermediates observed by each group were not seen by the other. Each group proposed destruction mechanisms for DMMP that formed a basis for further mechanism development. Aside from species profiles, Korobeinichev et al. also inferred changes in adiabatic flame speed by observing how maximum flame temperature varied with DMMP loading. They found that that under 5000 ppm, adding DMMP increases the flame speed, and above this concentration, the opposite holds in low-pressure H_2/O_2/Ar flames. More recently, Korobeinichev et al. [9] performed experiments in a premixed CH_4/O_2/Ar flame at 0.1 bar with a different organophosphorus compound, trimethyl phosphate. In contrast to their experiments with trimethyl phosphate [4,6] and DMMP [3,5] in hydrogen flames, these experiments showed an inhibitory effect on the flame.

Flame inhibition and suppression effects of DMMP and other organophosphorus compounds have been observed in non-premixed opposed-jet hydrocarbon flames, both through extinction measurements [17,18] and through measurements of flame radical levels [19]. They have also been seen in premixed flames by measuring the heat loss from the flame to a Bunsen burner [20]. Flame suppression effectiveness decreases as temperature increases [18, 19], and appears to be greatest under near stoichiometric conditions [20]. There is some agreement on the likely mechanism of flame inhibition by DMMP: phosphorus-containing radicals that are produced from DMMP at flame temperatures participate in catalytic cycles resulting in the recombination of standard flame radicals such as H and OH [15,21–23].

In the current work, the structure of a $CH_4/O_2/N_2$/Ar premixed flame doped with DMMP is studied at near-atmospheric pressure. Only stable species not containing phosphorus are measured. The impact of phosphorus on the flame is studied by comparing the undoped with doped profiles of the observable species.

2. Experimental apparatus and methods

2.1. Burner and gas flows

Experiments were conducted using a brass flat-flame burner resembling the one used by Korobeinichev et al. [3–9]. Further details on the apparatus and experimental technique are provided by Nogueira [24]. In the burner, the premixed reactants enter a the plenum from the bottom of the burner, flow upward through a bed of 3-mm-diameter glass beads, and then pass through an array of hexagonally spaced 0.58-mm diameter holes with center-to-center spacing of 0.95-mm holes in the upper surface of the burner. The use of a perforated plate, rather than a sintered metal plug, makes it possible to clean phosphorus-containing products from the burner. The diameter of the flow region is 53.4 mm, and the thickness of the brass plate is 6.35 mm. Surrounding the plenum is an annular passage through which cooling water flows. A centrifugal pump and resistance heater keep the cooling water, at 91°C, flowing at a rate slightly above 0.3 ml/min through a closed circuit including the water channel of the burner, a rotameter, and an annulus surrounding the reactants gas flow line.

Measurements at different heights were obtained by moving the burner relative to sampling probes or thermocouples. This burner was mounted on a motorized linear motion feedthrough, which is controlled by a programmable stepping motor. This device allows vertical movement with steps of 0.008 mm over a range of 100 mm. The repeatability of returning to a position is ± 0.08 mm. The burner and the traverse are sealed within a vertical stainless steel cylinder with 146-mm ID that serves as a vacuum chamber.

Gaseous reactants (CH_4, O_2, N_2, and Ar) are metered with calibrated mass flow controllers and meters. Upstream of the location where the nitrogen mixes with the other gases, liquid DMMP is introduced via a syringe pump (model A with 25-ml Hamilton Syringe; Razel, Stanford, CT). Downstream of the injection point, a chamber with a residence time of 12 s smoothes out fluctuations in the DMMP loading. The electrical heating and cooling water jacket maintain all reactant streams containing DMMP above 85°C, high enough to avoid DMMP condensation.

Table 1
Probe orifice diameters (μm) used in specific experiments

	Rich flame	Near-stoichiometric flame
Doped	61, 66	60, 65
Undoped	56, 67	59, 64

The vacuum chamber pressure is measured at the exhaust line downstream of the vacuum chamber by a capacitance pressure gauge (model PDR-C-1C; MKS, Andover, MA), calibrated using a "U" mercury manometer. Subatmospheric pressure is maintained by a reciprocating vacuum pump, and controlled by a butterfly valve. Fine tuning of the vacuum chamber pressure was obtained by raising or lowering a nitrogen shroud flow, which enters the bottom of the vacuum chamber without passing through the burner. Between the butterfly control valve and the vacuum pump in the vacuum chamber exhaust line is a cold trap using a bath of a mixture of a dry ice and acetone at 200°K, designed to remove phosphorus containing compounds and water from the exhaust stream. Safety considerations dictated the use of the vacuum chamber and subatmospheric operating conditions.

2.2. Sampling

Sampling for species and temperature measurements made use of a stationary quartz microprobe. The probe was 200 mm long and constructed of 6.0-mm OD, 3.8-mm ID quartz tubing, tapering to an orifice with a diameter ranging between 56 and 67 μm. Probe diameters were measured before each experiment. Specific probe orifice diameters used in the different experiments are listed in Table 1. Note that repeatability experiments performed on different days involved probes of different diameters; thus two probe diameters are listed for each flame condition. Downstream of the orifice is a 20-mm long vertically oriented section diverging with an angle of 11 degrees. In the following 25 mm, the probe undergoes a smooth 90° bend to a horizontal orientation, allowing it to be mounted in a sampling port in the side of the vacuum chamber.

The gases flowed through the probe, lengths of perfluoroalkoxy tubing, a gas cell, and a needle valve, and into a vacuum pump. The pressure downstream of the probe was kept under 150 torr to guarantee choked flow at the probe's orifice. A 50 SFM bubble flow meter (SGE International PTY LTD, Australia) was used to measure the volumetric flow rate through the probe. The bubble meter was located downstream of the small vacuum pump, where the flow pressure and temperature are close to room conditions. Depending upon the gas temperature and orifice size, between 15 and 45 min was needed to fill the FTIR cell with the gas sample.

Table 2
FTIR detectability limits and wavenumber ranges

Species	Wavenumber range used for quantification (cm^{-1})	Detectability limit[1]
CH_4	3176–3133	400
CH_2O	2920–2870	100[2]
CH_3OH	1060–1010	10
CO	2220–2030	1350
CO_2	715–670	1200
C_2H_6	3000–2950	70[2]
C_2H_4	960–905	60
C_2H_2	740–710	10

[1] A lower detectability limit could be achieved with a different choice of spectral region for many species.
[2] Quanitified after subtraction of CH_4 and CH_3OH.

2.3. Species measurements

FTIR measurements were taken with a Mattson RS-1 FTIR, in the wavelength range 500 to 4000 cm^{-1} with a resolution of 1 cm^{-1} and signal gain of 4. For these measurements, the sample gases flow continuously through an 884-ml multipass White cell (Infrared Analysis, Madison, WI) with gold-coated mirrors, zinc selenide windows, and a path length of approximately 5.4 m. The cell was maintained near 120 torr during data acquisition, and was purged and conditioned with gas flow between samples. The scanning time for the FTIR to obtain a sample spectrum was 7.2 min.

Gas-phase and volatile infrared-active species in the sample were quantified using an interactive subtraction technique that compares sample spectra to calibration spectra with known species concentrations. Spectral regions were chosen to minimize overlap, but in some cases interfering species had to be subtracted from the spectrum before quantification. Table 2 lists of spectral regions and sensitivities.

Radicals could not be measured with this technique because radical lifetimes were too short to persist through the sampling system. Although spectral features associated with DMMP and some of its phosphorus-containing products were observed, their levels were not repeatable. Previous research with extractive FTIR of organic phosphates and phosphonates and their pyrolysis products [10–12], suggests that the bulk of the lower-vapor-pressure products are lost by deposition on the surfaces upstream of the FTIR cell. DMMP itself should reach the gas cell, but at the low flow rates of the current experiments,

transients associated with wall adsorption and desorption result in a prohibitively long conditioning time requirement for reliable measurements. Reactions of DMMP and other species in the probe (see next section) also pose problems in obtaining quantitative species profiles. O_2, N_2, and H_2 are not detectable via IR absorption.

2.4. Probe effects

The choking at the probe orifice was experimentally verified by measuring flowrates of post-flame gases through the probe while varying the back pressure in the sampling system. The flowrate did not vary as long as the back pressure was below 190 torr, confirming that flow was choked under sampling conditions.

Literature correlations [25] indicate that the location from which gases are sampled should be approximately 3 orifice diameters, or 0.18 mm, upstream of the probe tip location. However, this is largely irrelevant to the comparison between calculated and experimental profiles, as the calculated profiles are based on temperatures measured a choked-probe technique that entails the same location error, as described below. Within 10 orifice diameters, or 0.6 mm, of the burner surface, surface/probe interactions lead to sampling of gas from both *downstream* and upstream of the probe [26]. This effect can be seen in the overrepresentation of products and under-representation of methane in samples taken near the burner surface.

Experiments with varying back pressure and with different probe designs were performed to assess the extent of reactions inside the probe [24]. In these experiments, dependence of species concentrations on the gas residence time in the hot region of the probe was seen as evidence for probe reactions. For undoped flames, the main distortion introduced by the probe was in the post-flame zone, where some conversion of CO to CO_2 was seen. In the flame zone, C_2H_2 was the only species affected by a factor of two reduction in residence time: its concentration dropped by a factor of two. For the preheat and flame zones of doped flames, there was evidence of very significant probe reactions involving CH_2O. All other species changed concentrations by less than a factor of 1.5 when the probe residence time was lowered by a factor of two (flame zone) or three (preheat zone). Many species concentrations were unchanged, and only CH_3OH changed by more than a factor of 1.3. Under the same conditions, CH_2O concentrations dropped by factors of 4 and 11, respectively, in the flame and preheat zones when residence time was reduced. It appears that DMMP conversion to CH_2O by probe reactions is significant in the pre-heat zone. Although CH_2O measurements in this region are not representative of flame concentrations, they can be used as an indicator of the presence of DMMP, as discussed below.

2.5. Temperature measurements

Temperatures in the flame zone were measured using the choked probe technique described by Kaiser et al. [26–28]. In this method, measured flowrates through the choked probe are compared to those obtained under reference conditions with known upstream temperature. Approximating the flow as one-dimensional and inviscid, the ratio of unknown to reference temperature is obtained. Two different reference conditions were used: (1) room conditions, and (2) post-flame conditions, where the temperature was measured with a platinum/platinum-rhodium thermocouple and corrected for radiative losses. Calculations based on the two different reference conditions yielded the temperatures that differed by less than 4%. Approximations to fluid properties are estimated to introduce errors between −1% and + 2%, depending on the location in the flame [24]

2.6. Materials

The following chemicals were used as reactants: CH_4 (99.99%), O_2 (99.994%), N_2 (99.998%), and Argon (99.998%) were bought from MG Industries (Malvern, PA) and used in the experiment as is. Dimethyl methylphosphonate (97%) was bought from Aldrich Chemical Co. (Milwaukee, WI) and used as is. To prepare calibration curves to quantify the FTIR results, the following gases were used: CO (99.5%), CO_2 (99.99%), C_2H_2 (99.6%), C_2H_4 (99.9%), and C_2H_6 (99.0%). All were bought from MG Industries (Malvern, PA), and used as is. Certified methanol (99.9%) was bought from Fisher Scientific (Fair Lawn, NJ) for the methanol calibration curve. A solution of formaldehyde (37%) with methyl alcohol (14%) and water (47%) was bought from Mallinckrodt Baker (Phillipsburg, NJ) for the formaldehyde calibration curve.

2.7. Operating conditions

Table 3 shows the operating conditions used in the current work. Four flames in all were studied: fuel-rich doped and undoped, and near-stoichiometric doped and undoped. Doping refers to the addition of a small quantity of DMMP. As can be seen from the table, reactant flowrates were chosen to match or nearly match several parameters: the reactants' cold flow velocity, the loading of DMMP for the doped cases, the ratio of inerts (N_2 and Ar) to O_2, and the

Table 3
Operating conditions

		Fuel-rich flames	Near-stoichiometric flames
Equivalence ratio		1.13	0.95
Flowrates (slpm)	CH_4	1.61	1.37
	O_2	2.84	2.88
	N_2	12.48	10.80
	Ar	0	1.94
	DMMP	9.18E-3 (doped), or 0(undoped)	9.18E-3 (doped), or 0 (undoped)
Ratio of $Ar+N_2$ to O_2		4.39	4.42
Cold flow velocity (cm/s)		12.6	12.6
Mole fraction DMMP in doped cases (ppm)		540	540
Adiabatic flame temperature (K)		2093	2139
Pressure (torr)		700	700
Inlet gas temperature (K)		376	373

adiabatic flame temperature. In addition, the chamber was at the same pressure and essentially the same inlet gas temperature for all measurements. Within these constraints, conditions were chosen by trial and error to provide a significantly lifted, yet non-cellular flame when DMMP was present.

3. Computational method

Premixed flame calculations were performed using the CHEMKIN suite of programs [29]. The steady laminar flame calculations used detailed chemical kinetics (described below) with mixture-averaged species diffusivities. Thermal diffusion was neglected. Temperature profiles were specified as their measured values.

Two chemical kinetic mechanisms for DMMP combustion were used, referred to in this work as the Babushok[1] [15] and Glaude [16] mechanisms. The mechanisms have in common the mechanism for destruction for small phosphorus compounds developed by Twarowski [21–23] but they differ somewhat in the paths for DMMP conversion into the small phosphorus containing species. The Babushok mechanism has 32 species and 199 elementary reactions. Many Arrhenius parameters here came from Werner and Cool's work. In the Werner-Cool mechanism, there some were estimates by the authors, and some heats of formation and activation energies were evaluated by BAC-MP4 calculation. The Werner-Cool mechanism for DMMP destruction was validated with relative species profile measurements from a low-pressure $H_2/O_2/Ar$ premixed flame at 50 torr [2], and the Babushok mechanism was validated with data from opposed-flow propane/air flames at 650 torr [15]. Glaude's mechanism for DMMP combustion has 43 species and 537 elementary reactions. It too is based on the work of Twarowski, Melius, and Werner and Cool, but includes new initial reactions for DMMP destruction. It was validated against Korobeinichev's low-pressure premixed flame results [3–6]. Korobeinichev and coworkers [7] have also recently proposed an updated kinetic mechanism using the mechanisms of Twarowski and Werner and Cool as their starting point. This mechanism was not evaluated in the present work.

Each of the DMMP combustion mechanisms was combined with the GRI 3.0 methane combustion mechanism [31], from which nitrogen chemistry had been removed. Nogueira [24] describes a series of calculations for which GRI 3.0 results were compared to those of a different methane combustion mechanism [32]. GRI 3.0 was selected because it was more successful in reproducing our experimental results for undoped flames, especially for methanol profiles.

4. Results and discussion

4.1. Temperature profiles

Figure 1 shows the temperature profiles obtained with and without DMMP doping. Measurements include duplicate data points taken on different days to ascertain repeatability. Choked flow measurements were processed using room conditions as a reference. Post-flame temperatures measured by thermocouple are presented for comparison. In all cases, the lowest measured temperature is about 250°K higher than that of the reactant stream. This is likely to be a result of the probe/burner interaction near the burner surface, resulting in sampling from both upstream and downstream of the probe orifice.

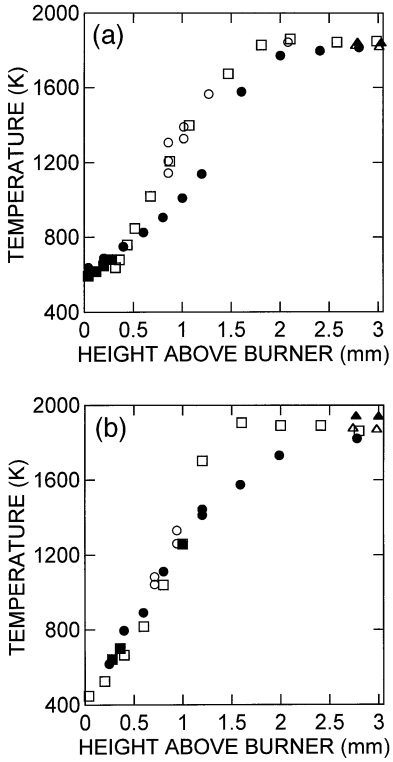

Fig. 1. Temperature profiles measured in (a) rich and (b) near-stoichiometric flames. Doped flames have filled symbols, while undoped flames have open symbols. Filled symbols: experimental data from doped flames; open symbols: experimental data from undoped flames; Squares were taken with the choked flow technique with a larger probe; circles were taken with the choked flow technique with a smaller probe (see Table 1 for sizes). Triangles were taken with thermocouples.

Both profiles have the same trend. Near the burner surface, doped and undoped temperatures are nearly the same, with doped slightly higher than undoped. The doped temperature increases less rapidly than the undoped one in the early part of the flame, and then increases more rapidly to achieve approximately the same post-flame value as the undoped case.

The shift of DMMP-doped flames away from the burner surface, seen in Fig. 1, can be interpreted by considering the heat transfer interaction between the flame and the burner surface. As there is a negligible change in cold velocity with doping, the change in position indicates that less heat transfer is required to stabilize the doped flame at a given velocity than is required for the corresponding undoped flame. This difference implies that the adiabatic flame speed of the doped mixture is lower than that of the undoped one, or that the overall reaction rate is slowed by the addition of DMMP. This conclusion is consistent with observations of flame-suppression effects of organophosphorus compounds in non-premixed methane flames [17–19]. In the absence of a change in adiabatic flame temperature with doping, the flame shift away from the burner should lead to less heat loss and thus a higher post-flame temperature in the doped case. Under our conditions, thermocouple measurements suggest that this is a small effect. Temperatures measured by the choked-orifice method are similar for doped and undoped cases at the highest sampling location, but the undoped flame is actually slightly hotter. However, the shape of the curves suggests that the final post-flame temperature has not been reached for some profiles at that location, leading to uncertainty in the final temperatures.

The shift away from the burner, or broadening of the reaction zone, is consistent with the results of Korobeinichev et al. for trimethyl phosphate in a CH_4/O_2/Ar flame at 0.1 bar [9]. The lack of significant effect of the additive on final temperature however, is different from Korobeinichev's observations, which indicated that doped final temperatures exceed the corresponding undoped ones by about 200°K. Korobeinichev et al. attributed this higher temperature to the lower heat loss and more complete combustion in the doped case. As observed by Korobeinichev [9], organophosphorus additives have a distinctly different effect on lower-pressure hydrogen flames, narrowing the reaction zone and raising the final temperature by 350 to 450°K [2–4]. This change from promotion to inhibition behavior is predicted by low-pressure flame speed calculations performed by Korobeinichev and coworkers [9], who offer a qualitative explanation for it based on the effect of radical termination reactions on the heat release rate. Korobeinichev and co-workers [9] observe that the inhibitory behavior of organophosphorus compounds increases with pressure, and is greater in methane than in hydrogen flames. The current experiments, performed at still higher pressures, confirm this trend.

4.2. Comparison of doped and undoped profiles

Figures 2 through 9 are species profiles for the eight measured species. Each profile shows undoped and doped experimental results (symbols), along with computational results (lines). In each figure, the dashed line is the undoped calculation using the GRI 3.0 mechanism, while the dotted and solid lines are the doped calculations with Glaude and Babushok mechanisms, respectively. Each profile includes some data points acquired on a different day, with a different probe orifice diameter, as indicated in the figure captions.

Doping the flame shifts all species profiles down-

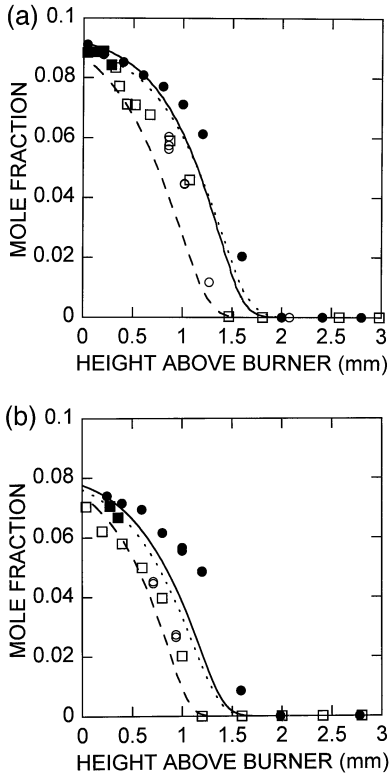

Fig. 2. CH_4 in doped and undoped (a) rich and (b) near-stoichiometric flame, with GRI (undoped) and Babushok and Glaude (doped) predictions. Filled symbols: experimental data from doped flames; open symbols: experimental data from undoped flames; Squares were taken with a larger probe; circles were taken with a smaller probe (see Table 1 for sizes). Dashed line: GRI prediction; solid line: Babushok prediction; dotted line: Glaude prediction.

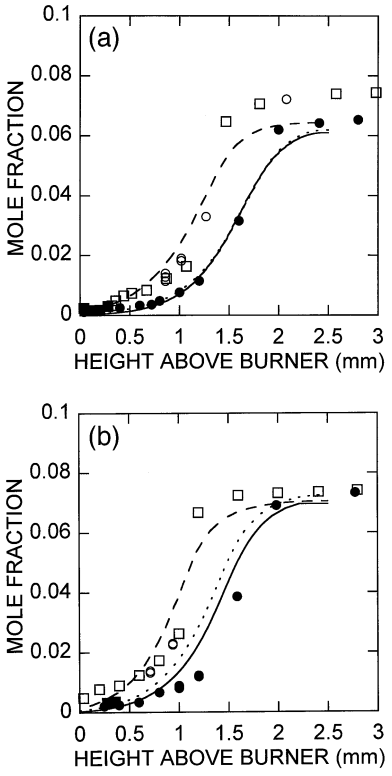

Fig. 3. CO_2 in doped and undoped (a) rich and (b) near-stoichiometric flame, with GRI (undoped) and Babushok and Glaude (doped) predictions. Filled symbols: experimental data from doped flames; open symbols: experimental data from undoped flames; Squares were taken with a larger probe; circles were taken with a smaller probe (see Table 1 for sizes). Dashed line: GRI prediction; solid line: Babushok prediction; dotted line: Glaude prediction.

stream, similar to the behavior of the temperature as described above. The magnitude of this shift is best evaluated from the monotonic CH_4 or CO_2 profiles, as the axial spacing of sampling locations is too large to allow reliable comparisons of peak locations for intermediate species. These profiles were fitted to a scaled Weibull cdf form to reduce the impact of noise. Defining the shift as the change in position in the curvefit where half the initial methane is consumed, the experimental values are 0.33 and 0.49 mm for the rich and near-stoichiometric flames, respectively. Similarly, using the location where CO_2 reaches half its maximum value, the experimental shifts are 0.34 and 0.53 mm, respectively. Thus, DMMP consistently has a larger effect on flame location for the near-stoichiometric than for the rich flame under these conditions, and defining flame position in terms of fuel or product profiles yields similar shifts.

The sampling technique produces artifacts in some profiles, most notably CH_2O. For this species, two peaks can be seen in each of the experimental doped profiles, while the undoped experimental profiles and all the computational profiles show single peaks. The earlier doped peak occurs 0.25 mm from the burner for both equivalence ratios, and appears to be due to probe reactions. The location of the first peak close to the burner surface suggests that the upstream peak comes directly from DMMP destruction, but the low temperatures (<700°K) and presumed low radical levels there imply that destruction of significant quantities of DMMP in the free stream is very unlikely [33]. The magnitude of this peak increases strongly with probe residence time, as shown in the back pressure experiments described in the previous section. The current data set shows further evidence of this dependence: The highest values of CH_2O in Fig. 5 were repeat data points measured using slightly smaller probe orifice diameters than the other data points (see Table 1 for orifice diameters).

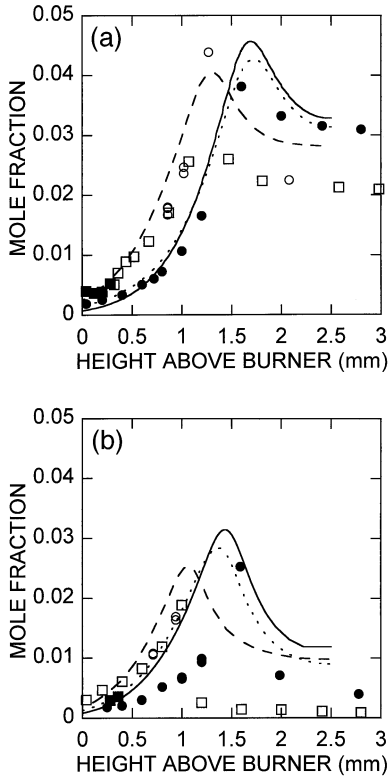

Fig. 4. CO in doped and undoped (a) rich and (b) near-stoichiometric flame, with GRI (undoped) and Babushok and Glaude (doped) predictions. Filled symbols: experimental data from doped flames; open symbols: experimental data from undoped flames; Squares were taken with a larger probe; circles were taken with a smaller probe (see Table 1 for sizes). Dashed line: GRI prediction; solid line: Babushok prediction; dotted line: Glaude prediction.

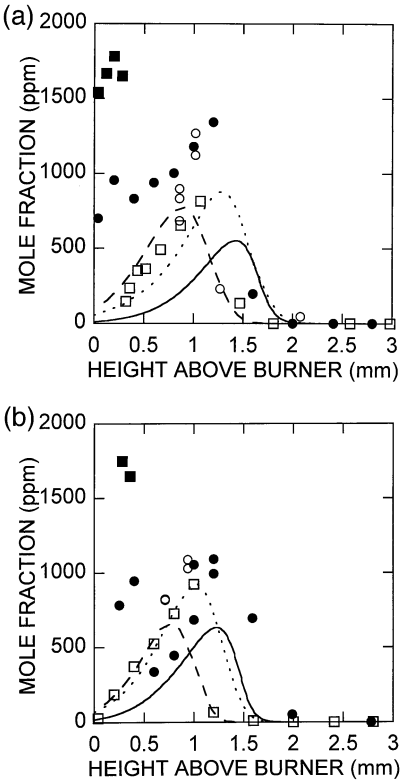

Fig. 5. CH_2O in doped and undoped (a) rich and (b) near-stoichiometric flame, with GRI (undoped) and Babushok and Glaude (doped) predictions. Filled symbols: experimental data from doped flames; open symbols: experimental data from undoped flames; Squares were taken with a larger probe; circles were taken with a smaller probe (see Table 1 for sizes). Dashed line: GRI prediction; solid line: Babushok prediction; dotted line: Glaude prediction.

The points taken with the smaller probe orifice (and corresponding longer residence time in the probe with choked flow) have much higher CH_2O levels than the points taken with the larger probe orifice. Although it is a sampling artifact, this upstream CH_2O peak can provide information about the DMMP profile. The drop in CH_2O levels at 0.25 mm above the burner indicates that DMMP levels in the gas stream entering the probe begin to drop at this location.

For most intermediates, there is no clear change in peak height due to doping. The measured peak height changes with doping by about a factor of two for C_2H_2, about a factor of 1.5 for CO and for the second peak of CH_2O, and by smaller amounts for C_2H_4 and C_2H_6. In each of these cases, a narrow peak along with limited spatial resolution makes it hard to determine whether the true height has been sampled.

CH_3OH levels, on the other hand, show a dramatic change in peak height with doping, increasing by factors of seven and four for the rich and near-stoichiometric cases, respectively. The broad peak shape (see Fig. 9) greatly reduces uncertainty due to limited spatial resolution of sampling. Accounting for probe reactions would only increase the difference between doped and undoped profiles, as can be seen from the doped data points taken with smaller probe orifice size (longer residence time). Werner and Cool [2] did not measure methanol and formaldehyde because the energy needed for their ionization was above the capability of their apparatus. Korobeinichev and co-workers [3,5] did not report profiles for these species.

4.3. Comparison between Experimental and Computational Profiles

Figures 2 through 9 also show how successful the two chemical kinetic mechanisms for phosphorus

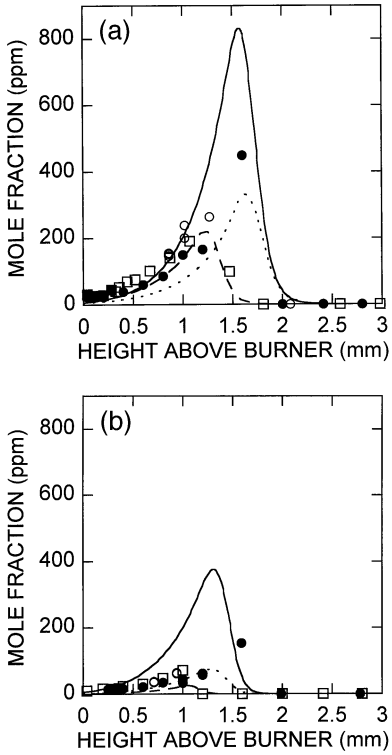

Fig. 6. C_2H_2 in doped and undoped (a) rich and (b) near-stoichiometric flame, with GRI (undoped) and Babushok and Glaude (doped) predictions. Filled symbols: experimental data from doped flames; open symbols: experimental data from undoped flames; Squares were taken with a larger probe; circles were taken with a smaller probe (see Table 1 for sizes). Dashed line: GRI prediction; solid line: Babushok prediction; dotted line: Glaude prediction.

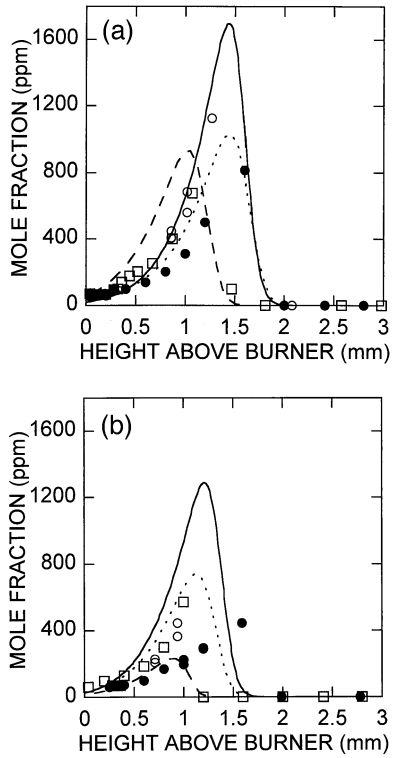

Fig. 7. C_2H_4 in doped and undoped (a) rich and (b) near-stoichiometric flame, with GRI (undoped) and Babushok and Glaude (doped) predictions. Filled symbols: experimental data from doped flames; open symbols: experimental data from undoped flames; Squares were taken with a larger probe; circles were taken with a smaller probe (see Table 1 for sizes). Dashed line: GRI prediction; solid line: Babushok prediction; dotted line: Glaude prediction.

combustion (Babushok and Glaude) are at duplicating experimental data in doped flames. (The first experimental CH_2O peak is excluded from the comparison below as it is considered a sampling artifact.) It is convenient to use the GRI mech predictions of undoped species profiles as a benchmark. By some qualitative measures, the phosphorus mechanisms are as successful as the GRI mechanism: All mechanisms successfully predict the direction of change in peak height when the equivalence ratio changes from rich to near-stoichiometric for CH_2O, CO, C_2H_2, and C_2H_4, and all mechanisms fail for C_2H_6. For CH_3OH, GRI fails while the Babushok and Glaude mechanisms succeed. None of the mechanisms succeed in predicting the ranking of peak heights in a particular doped or undoped flame.

More quantitatively, in predicting peak heights, the Glaude mechanism (for doped flames) is roughly equally successful to the GRI mechanism (for undoped flames). Glaude's fractional differences in peak height between experiment and calculation are smaller than or about the same magnitude as the corresponding GRI values for all species except CH_3OH. Babushok's mechanism is less successful, producing larger fractional differences than GRI for all cases except C_2H_6 in the near-stoichiometric flame and CO in both flames. In the case of overpredictions, for example C_2 predictions with Babushok's mechanism, these discrepancies must be viewed with some caution because true peaks may not be sampled experimentally. Another explanation for some differences is probe reactions, which can produce changes of 30% or so in most species concentrations in the flame zone, as described above. The discrepancies between experiment and calculations with the Babushok mechanism clearly exceed errors due to probe reactions (i.e., exceed the observed sensitivity to probe residence time) only for C_2H_2, C_2H_4, and CH_3OH.

Methanol computational results show large discrepancies with experiment for both phosphorus

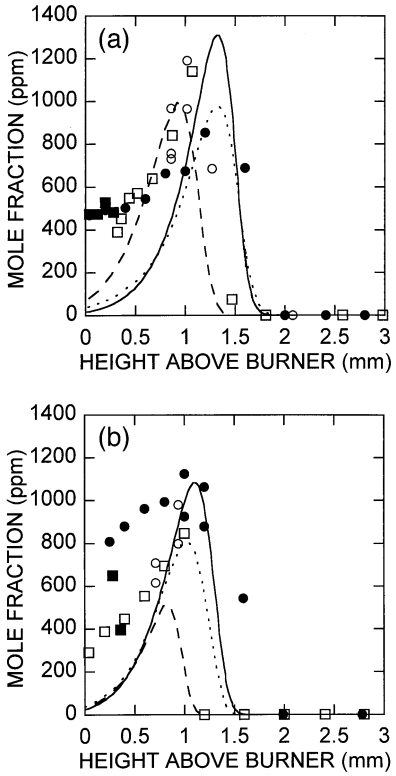

Fig. 8. C_2H_6 in doped and undoped (a) rich and (b) near-stoichiometric flame, with GRI (undoped) and Babushok and Glaude (doped) predictions. Filled symbols: experimental data from doped flames; open symbols: experimental data from undoped flames; Squares were taken with a larger probe; circles were taken with a smaller probe (see Table 1 for sizes). Dashed line: GRI prediction; solid line: Babushok prediction; dotted line: Glaude prediction.

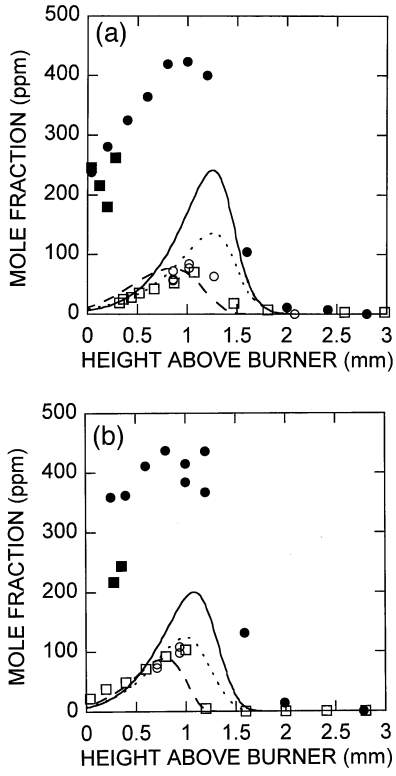

Fig. 9. CH_3OH in doped and undoped (a) rich and (b) near-stoichiometric flame, with GRI (undoped) and Babushok and Glaude (doped) predictions. Filled symbols: experimental data from doped flames; open symbols: experimental data from undoped flames; Squares were taken with a larger probe; circles were taken with a smaller probe (see Table 1 for sizes). Dashed line: GRI prediction; solid line: Babushok prediction; dotted line: Glaude prediction.

combustion mechanisms. Qualitatively, the mechanisms succeed in predicting that the doped CH_3OH peak is higher than the undoped peak. However, they predict the peak to be too narrow and located too far downstream, and they substantially underpredict its height. Babushok and Glaude mechanisms predict that the CH_3OH peak height increases, respectively, by factors of 1.4–1.8 and 2.2–3.2, over the undoped calculated values. The experimental increase is by factors of 4 (near-stoichiometric) and 7 (rich). This difference indicates an area in which improvements to both mechanisms are needed. The early location of the start of the doped CH_3OH peaks suggests that CH_3OH is an important intermediate in the early decomposition process for DMMP.

Both phosphorus mechanisms agree with experiments in predicting that doping produces a downstream shift of species profiles. The magnitude of the shift is similar for the two mechanisms, an expected result, as calculations with both mechanisms make use of the same specified experimental temperature profiles. The two calculations predict almost identical shifts in the rich case for all species. In the near-stoichiometric flame, the shift is somewhat larger for Babushok than for Glaude, especially for CH_2O. With the measures of shift size based on the position where CH_4 concentration is half of the initial concentration as described in the previous section, Glaude and Babushok give almost identical shifts for the rich case, while Babushok's shift is 30% larger in the near-stoichiometric flame. In comparison to experimental shifts, calculations are about 20% too large in the rich flame, and about 45% too small in the near-stoichiometric flame. Both mechanisms fail to predict that the shift in the near-stoichiometric flame is greater than the one in the rich flame. The magnitudes of the shifts are predicted slightly better by Babushok than by Glaude.

It is important to note that in the current work Glaude's and Babushok's phosphorus mechanisms

are combined with the same methane combustion mechanism (GRI 3.0). It is possible that either mechanism would make more successful predictions when used with the methane combustion mechanism with which it was developed.

5. Summary and conclusions

A facility has been developed for the study of premixed hydrocarbon flames doped with a small quantity of a low-vapor-pressure organophosphorus compound, DMMP. The burner performed satisfactorily, but the probe sampling technique produced artifacts in profiles of certain species. This facility was used to examine the effect of DMMP doping on two flames with similar undoped temperature profiles, one with equivalence ratio 1.13 (rich), and the other with equivalence ratio 0.95 (near-stoichiometric).

When DMMP was added to the rich or near-stoichiometric flame, there was a shift in the downstream direction of temperature profiles and all species profiles except CH_3OH. This shift is a consequence of the flame inhibition properties of the DMMP additive: decreases in the overall reaction rate with doping lead to flame stabilization farther from the burner surface. The magnitude of the shift was over 50% greater for the near-stoichiometric flame than for the rich flame. Flame calculations were performed with two detailed chemical kinetic mechanisms for organophosphorus combustion, referred to here as the Babushok and Glaude mechanisms. Each of these mechanisms was combined with the GRI 3.0 methane combustion mechanism. The two mechanisms are reasonably successful in predicting the effects of DMMP on the flame. They predict downstream shifts in species profiles, though both mechanisms predict a larger shift for the rich flame than for the near-stoichiometric one. The Glaude mechanism predicts peak heights for the doped flame as well as the GRI mechanism does for the undoped flame, with the exception of CH_3OH profiles.

Experimental CH_3OH profiles were much higher in the doped flames than in the doped ones. Both mechanisms substantially underpredicted the magnitude of the increase in peak height with doping. Further mechanism development is needed here.

Notes

1. This mechanism available from its author and is also listed in a Ph.D. thesis making use of it [30].

Acknowledgments

The authors thank Dr. Valeri Babushok (NIST) and Dr. Pierre Glaude (Lawrence Livermore Laboratory) for numerous useful discussions on chemical kinetics, and for making their mechanisms available before publication. They also thank Prof. F. C. Gouldin (Cornell), Dr. E. William Kaiser (Ford), and Prof. Oleg Korobeinichev (Siberian Branch, Russian Academy of Sciences) for helpful recommendations on the experimental technique. MFMN acknowledges the financial support of the Fundação Coordenação de Aperfeiçoamento de Pessoal de Nível Superior – CAPES and the Department of Mechanical Engineering of the Universidade Federal do Pará during his Ph.D. studies. The assistance of Mr. Sean O'Brien in conducting experiments is appreciated.

References

[1] R. Rife, T.W. Thomas, D.W. Norberg, R. Fournier, F.G. Rinker, M.S. Bonomo, Environm. Progr. 8 (1989) 167.
[2] J.H. Werner, T.A. Cool, Combust. Flame 117 (1999) 78.
[3] O.P. Korobeinichev, S.B. Il'in, V. Mokrushin, A.G. Shmakov, Combust. Sci. Technol. 116,117 (1996) 51.
[4] O.P. Korobeinichev, V.M. Shvartsberg, A.A. Chernov, V.V. Mokrushin, Twenty-Sixth Symposium (International) on Combustion, The Combustion Institute, Pittsburgh, 1996, p. 1035.
[5] O.P. Korobeinichev, S.B. Ilyin, V.M. Shvartsberg, A.A. Chernov, Combust. Flame, 118 (1999) 718.
[6] O.P. Korobeinichev, V.M. Shvartsberg, A.A. Chernov, Combust. Flame 118 (1999) 727.
[7] O.P. Korobeinichev, S.B. Ilyin, T.A. Bolshova, V.M.. Shvartsberg, A.A. Chernov, Combust. Flame 121 (2000) 593.
[8] O.P. Korobeinichev, A.A. Chernov, T.A. Bolshova, Combust. Flame 123 (2000) 412.
[9] O.P. Korobeinichev, T.A. Bolshova, V.M. Shvartsberg, A.A. Chernov, Combust. Flame 125 (2001) 744.
[10] E.J.P. Zegers, E.M. Fisher, Combust. Sci. Technol. 116–117 (1996) 69.
[11] E.J.P. Zegers, E.M. Fisher, Combust. Sci. Technol. 138 (1998) 85.
[12] E.J.P. Zegers, E.M. Fisher, Combust. Flame 115 (1998) 230.
[13] W.M. Pitts, M.R. Nyden, R.G. Gann, W.G. Mallard, W. Tsang, Construction of an Exploratory List of Chemicals to Initiate the Search for Halon Alternatives, NIST Technical Note 1279, 1990.
[14] J.A. Kaizerman, R.E. Tapscott, Advanced Streaming Agent Development, vol. III: Phosphorus Compounds, New Mexico Engineering Research Institute Report NMERI 96/5/32540, 1996.
[15] R.T. Wainner, K.L. McNesby, R.G. Daniel, A.W. Miziolek, V.I. Babushok, Proceedings of the Halon Op-

tions Technical Working Conference, 2000, pp. 141–153.
[16] P.A. Glaude, H.J. Curran, W.J. Pitz, C.K. Westbrook, Proc. Combust. Inst. 28 (2000) 1749.
[17] M.A. MacDonald, T.M. Jayaweera, E.M. Fisher, F.C. Gouldin, Combust. Flame 116 (1998) 166.
[18] M.A. MacDonald, T.M. Jayaweera, E.M., Fisher, F.C. Gouldin, Twenty-Seventh Symposium (International) on Combustion, The Combustion Institute, 1998, pp. 2749–2756.
[19] M.A. MacDonald, F.C. Gouldin, E.M. Fisher, Combust. Flame 124 (2001) 668.
[20] J. Riches, K. Grant, L. Knutsen, Laboratory Testing of Some Phosphorus-Containing Compounds as Flame Suppressants, presented at the 1999 Halon Options Technical Working Conference, Albuquerque, NM, April 27–29, 1999.
[21] A. Twarowski, Combust. Flame 102 (1995) 41.
[22] A. Twarowski, Combust. Flame 94 (1993) 91.
[23] A. Twarowski, Combust. Flame 94 (1993) 341.
[24] M.F.M. Nogueira, Effects of Dimethyl Methylphosphonate of Premixed Methane Flames, Ph.D. Thesis, Mechanical Engineering, Cornell University, Ithaca, NY, 2001.
[25] A. Yi, E.L. Knuth, Combust. Flame 63 (1986) 369.
[26] E.W. Kaiser, W.G. Rothschild, G.A. Lavoie, Combust. Sci. Technol. 33 (1983) 123.
[27] E.W. Kaiser, W.G. Rothschild, G.A. Lavoie, Combust. Sci. Technol. 41 (1984) 271.
[28] E.W. Kaiser, T.J. Wallington, M.D. Hurley, J. Platz, H.J. Curran, W.J. Pitz, C.K. Westbrook, J. Phys. Chem. A 104 (2000) 8194.
[29] R.J. Kee, F.M. Rupley, J.A. Miller, et al. Chemkin Collection, Release 3.5, Reaction Design, Inc., San Diego, CA, 1999.
[30] M.A. Macdonald, Inhibition of Non-Premixed Flames by Phosphorus-Containing Compounds, Ph.D. Thesis, Mechanical Engineering, Cornell University, 2000.
[31] G.P. Smith, D.M. Golden, M. Frenklach, N.W. Moriarty, B. Eiteneer, M. Goldenbarg, C.T. Bowman, R.K. Hanson, S. Song, W.C. Gardiner, Jr, V.V. Lissianski, Z. Qin, GRI Mech 3.0, 1999, http://www.me.berkeley.edu/gri mech/.
[32] V. Karbach, J. Warnatz, Proceedings of the 3rd International Workshop on Measurement and Computation of Turbulent Nonpremixed Flames, Boulder, CO, 1998, http://nathan.ca.sandia.gov/tdf/3rdWorkshop/ch4mech. html.
[33] E.J. Zegers, Pyrolysis of Alkyl Phosphates and Phosphonates, Ph.D. Thesis, Mechanical Engineering, Cornell University, Ithaca, NY, 1997.